ISBN: 978-3-95450-245-5 ISSN: 2226-0374 doi:10.18429/JACoW-COOL2023-FRPAM1R2

ELECTRON COOLING IN NICA ACCELERATION COMPLEX

A. Butenko, V. Lebedev†, I. Meshkov, K. Osipov, Yu. Prokopjechev, V. Shpakov, S. Semenov, A. Sergeev, E. Syresin, R. Timonin, G. Trubnikov
Joint Institute for Nuclear Research, Dubna, Russia
M. Bryzgunov, A. Bubley, V. Panasyuk, V. Parkhomchuk, V. Reva
Budker Institute for Nuclear Physics SB RAS, Novosibirsk, Russia

Abstract

The paper reports results of experimental studies of electron cooling carried out during commissioning of injection complex of NICA (the Nuclotron-based Ion Collider fAcility). Further plans of electron cooling developments and usage are also described.

NICA INJECTION COMPLEX

The Nuclotron-based Ion Collider fAcility (NICA) is in construction at JINR [1, 2]. The collider first beam tests are planned for the second half of 2024. The goal of the second stage of NICA project is to provide colliding beams for studies of collisions of heavy fully stripped ions at energies up to 4.5 GeV/u. The injection complex consists of two collider rings supporting head-on collisions in two interaction points and the injection complex [3, 4] which includes linac and two synchrotrons: Booster and Nuclotron. The injection complex is already in commissioning for few years. Stable operation of the complex has been achieved and different ion species were delivered to the BM@N and SRC experiments [5, 6] with slow beam extraction. By present time the ion beams of He, Fe, C [7] and Xe [8] were accelerated in these synchrotrons during four beam runs. With start of collider operation, the injection complex has to support both the collider operation and the fixed target experiments with slow extracted beams. Two particle detectors, a Multi-Purpose Detector (MPD) [9] and a Spin Physics Detector (SPD) [10], are located in two straight sections at the opposite sides of the collider.

The Krion-6T [11] ion source introduced into operation in Run IV will provide the beam of highly multicharged ions. $^{197}Au^{31+}$ and $^{209}Bi^{35+}$ ions are planned to be used in the collider operation. In Run IV (Sep. 2022 – Feb. 2023) we used Xe^{28+}. The same ions are expected to be used at the beginning of collider commissioning. In Run IV about a quarter of the ions extracted from the source had the targeted charge. A typical intensity was about 10^8 ions per pulse for the targeted charge. After electrostatic acceleration to 17 keV/u the beam is accelerated in the RFQ and 2 sections of heavy ion linac (HILAC) [12] to the energy of 3.2 MeV/u. Then the beam is injected into the Booster with single turn injection.

The Booster is a superconducting synchrotron designed to accelerate heavy ions to the energy of 600 MeV/u (A/Z≈6). At the Booster extraction the ions come through stripping foil where they are fully stripped and then are directed to Nuclotron for further acceleration to 3.9 GeV/u. The collider design report [3] requires the beam intensity of about 10^9 ions per injection complex pulse with cycle duration of ~4-5 s. The beam extracted from Nuclotron will be injected into collider rings where first it is accumulated in the barrier bucket RF, then bunched and brought to collisions.

The ion xenon beam extracted from Krion-6T had ~5 charge states with the targeted charge state (Z=28) taking about 25%. The peak of total ion beam current at the RFQ exit is about 200 μA (curve 1, Fig.1). Since there is considerable loss for the non-target states the total beam current is significantly reduced at the linac exit (curve 2, Fig. 1). With existing instrumentation, we cannot accurately measure the actual loss of the targeted state in the course of beam acceleration in the linac. Typically, the $^{124}Xe^{28+}$ion intensity corresponds to $5{\cdot}10^7$ ions at HILAC exit with total beam pulse duration of about 12-15 μs.

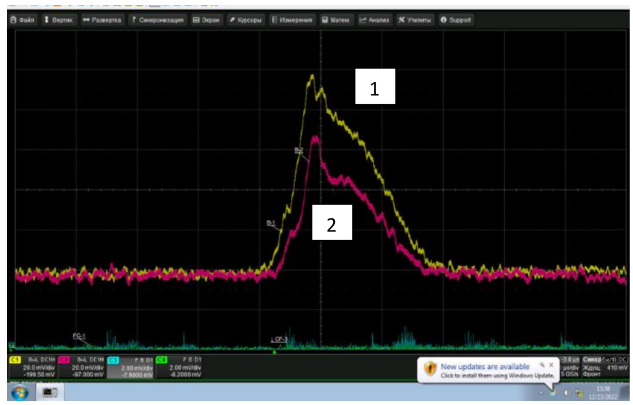

Figure1: Signals of current transformers at the RFQ exit (curve 1) and the HILAC exit (curve 2).

Curve 1 in Fig. 2 presents a typical magnetic cycle of the Booster. As one can see from curve 2, showing the beam current, the beam is injected at the first plateau, where it is adiabatically bunched at the 5th harmonic. Then the beam is accelerated to the second plateau corresponding the ion energy of 65 MeV/u, where it is adiabatically rebunched to the first harmonic. Finally, the beam is accelerated to the top energy of 205 MeV/u and extracted to Nuclotron. Typically, the accelerated to top energy $^{124}Xe^{28+}$ ions constitute about 60% of all ions at the linac exit.

Note that the electron cooling installations are important part of the accelerating complex. The first one is already installed and operates in Booster, and two others will be installed in each of the collider rings.

The intensity the of Xe^{28+} ion beam is expected to increase by a factor of 2 during next Booster Run. However,

† valebedev@jinr.ru

ISBN: 978-3-95450-245-5 ISSN: 2226-0374 doi:10.18429/JACoW-COOL2023-FRPAM1R2

this intensity still will be less than required for the collider by almost one order of magnitude [3]. To address this, we initially planned to accumulate the beam in the Booster transverse plane with multiple injections and beam damping with electron cooling [13]. Since the longitudinal cooling is faster, at the present time we plan an accumulation in the longitudinal plane.

The electron cooling in the Collider will be used for the beam accumulation and the suppression of intrabeam scattering during accumulation, bunching and collisions.

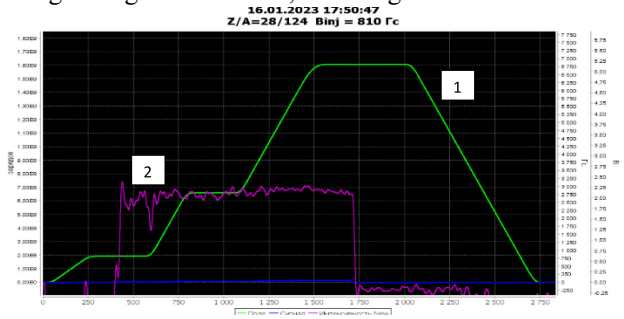

Figure 2: Magnetic field dependence on time for a typical Booster cycle (curve 1), and the number of particles in the beam measured with direct current transformer and normalized to account changes in particle velocity (curve 2); $^{124}Xe^{28+}$ions.

BOOSTER ELECTRON COOLING

The Booster electron cooling system [14-16] designed and manufactured by BINP SB RAS has the maximum electron energy of 60 keV and cooling length 2.5 m [3]. In the collider operations it will be used at the injection energy of 3.2 MeV/u for beam accumulation and cooling. Although the Booster electron cooling was tested with multiple ion species it was not routinely used in the beam delivery to users up to almost the end of Run IV.

Investigation of Booster electron cooling was done during the 2nd [4] and 4th [8] Runs. The measurements were produced at the injection energy of 3.2 MeV/n for $^{56}Fe^{14+}$ [4] (Fig. 3) and $^{124}Xe^{28+}$ions (Fig. 4).

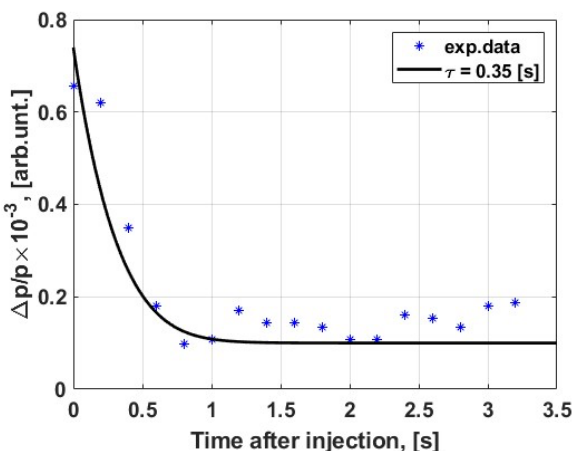

Figure 3: Dependence of ion momentum spread of $^{56}Fe^{14+}$ ion beam on time at the ion energy of 3.2 MeV/u and the electron beam current of 76 mA. The measurements were performed for continuous beam with Schottky noise.

During 4th Run the ion $^{124}Xe^{28+}$ acceleration was started in 0.23 s after beam injection. Although this is relatively short time it still was sufficient to provide cooling of ions with reduction of bunch time duration by a factor of 3 with the electron beam current of 50 mA (Figs. 4 and 5).

Dependences of bunch duration on time for cooling on (solid curve) and off (doted curve) are shown in Fig. 5. The comparison of these curves yields the longitudinal cooling time about 70 ms.

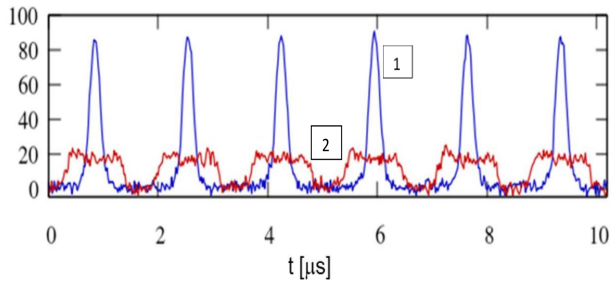

Figure 4: Longitudinal bunch profiles of $^{124}Xe^{28+}$ion beams without (curve 2) and with (curve 1) electron cooling. The electron beam current is 50 mA. The measurements were acquired with fast beam current monitor shortly before the beam acceleration in the presence of RF voltage.

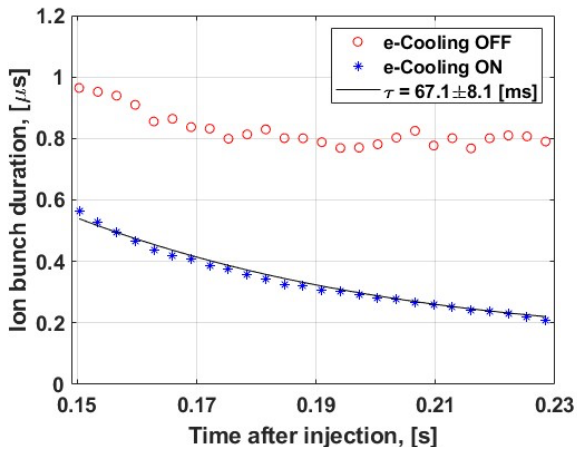

Figure 5: Dependence of bunch duration on time for cooling on (solid curve) and off (doted curve) measured in Run IV; $^{124}Xe^{28+}$ions.

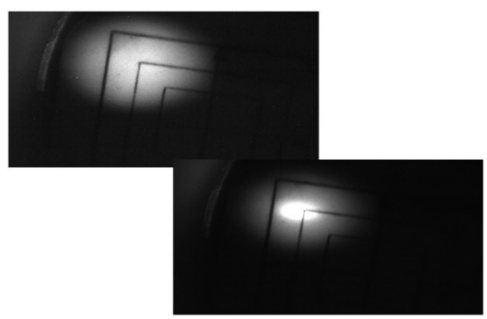

Figure 6: Transverse profiles of ion beam on the beam viewer (luminophore screen) without (upper) and with (down) cooling. The beam intensity was reduced to avoid saturation.

ISBN: 978-3-95450-245-5 ISSN: 2226-0374 doi:10.18429/JACoW-COOL2023-FRPAM1R2

An effect of transverse cooling was observed on a beam viewer installed in the Booster-Nuclotron transfer line. That allows one to acquire an image of transverse distribution for the beam intensity after its acceleration. As one can see in Fig. 6 the beam cooling reduces the FWHM beam transverse sizes from 7.81 mm and 5.38 mm to 3.34 mm and 1.63 mm for horizontal and vertical planes, respectively.

The reduction of beam emittances resulted in a reduction of beam loss with subsequent doubling in the intensity for the beam extracted from the Nuclotron to BM@N experiment. As result the number of $^{124}Xe^{54+}$ nuclei reached 10^7 per pulse (Fig. 7).

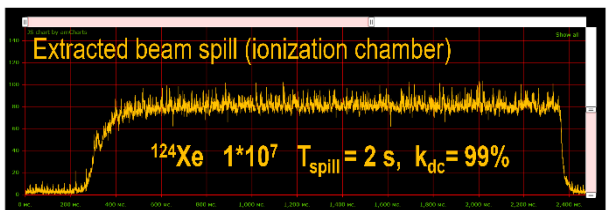

Figure 7: Dependence of beam intensity on time for the beam extracted from Nuclotron; $^{124}Xe^{54+}$ ions, extraction efficiency ~30%, coefficient k_{dc} characterizes time uniformity of extracted beam intensity.

BEAM ACCUMULATION IN BOOSTER

To support the collider operation, we need to increase the number of ions delivered to the Nuclotron top energy by a factor of 30, which is related to a lack of the intensity in the ion source by a factor 20 in comparison with the project value. It will be achieved by the ion accumulation in the Booster with help of electron cooling and by reduction of the beam loss during beam acceleration and transfers.

Since the longitudinal cooling is much faster than transverse, we choose the beam accumulation in the longitudinal plane. In this case about half of the Booster orbit is given to the accumulated bunch, and another half is assigned for the injected beam. The electron cooling has to free the injection space before next injection. Calculations, supported by the above presented results on electron cooling, determine the optimal stacking rate of about 10 Hz; and ~10-15 injections are required to obtain the beam population limited by the beam space charge at the injection energy. Thus about 1-1.5 s of 5-5.5 s acceleration cycle will be used for the beam accumulation in the Booster. A 10 Hz operation of KRION-6T ion source with 10 pulses was recently demonstrated with $^{124}Xe^{28+}$ ions. Better tuning of ion source resulted in an increase of total charge from 2.4 to 3 nC.

Next step in the ion source upgrade is aimed on shortening the pulse duration from ~15 μs (the total duration) to 4 μs. It will be achieved by changing shape of electrodes holding the ion column to make uniform extraction electric field. A special time program for powering the electrodes should additionally form rectangular pulse shape in time and decrease the energy spread of outcoming ions.

The low energy beam transport and powering of linac and transfer line quads were not originally built to support 10-15 linac pulses at 10 Hz operation. Therefore, a considerable number of hardware pieces has to be upgraded to withstand higher repetition rate. This work is already proceeding and we expect the linac upgrade to be complete by the end of 2023.

The beam accumulation in Booster will be done at the 1st RF harmonic. The RF bucket height of $(\Delta p/p)_{max} = 1 \cdot 10^{-3}$ was chosen to maximize the cooling rate. It requires the RF voltage of 200 V.

The half of Booster ring will be used for injection and other half for accumulation (Fig. 8). Each new injection happens after the previous one is cooled to the core. The permanently present 1st RF harmonic weakly affects high amplitude particles. The total number of accumulated ions and depth of the cooling are restricted by the ion bunch space charge. We expect to be able to store about 10^9 ions of $^{209}Bi^{35+}$.

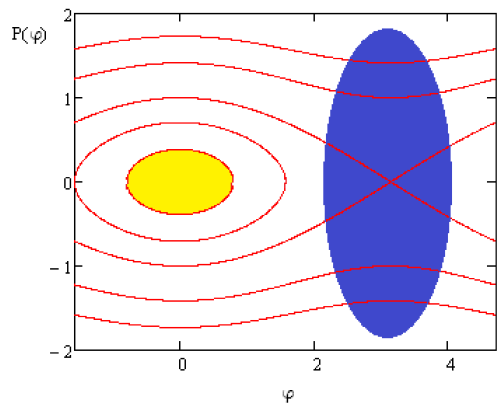

Figure 8: Sketch of Booster ion accumulation with electron cooling in longitudinal plane.

To minimize the longitudinal emittance growth, we plan to avoid rebunching in the course of beam acceleration in Booster. Thus, the entire acceleration will proceed at the first harmonic. Since at the accelerator cycle beginning the RF frequency is outside nominal operation frequency band the initial RF voltage will be lower (~1.5 kV). That lengthens the accelerating cycle by 300 ms – the time which otherwise will be spent for rebunching.

COLLIDER

The Collider [1-3, 7] consists of two storage rings with two interaction points (IPs). Its main parameters for operation with bismuth fully stripped ions are presented in Table 1. The collider rings have the same shape and are separated vertically. They have two arcs connected by two 109 m straight sections.

An installation of the magnetic elements of the Collider arcs began in December 2021. All dipole magnets and arc quads were assembled and tested on the cryogenic stand. Most of the arc magnets are installed in the Collider tunnel (Fig. 9). Four out of eight RF2 (22nd harmonic) and one out of two RF1 (barrier backet) systems are also installed. Installation of the remaining four RF2 systems and RF1 system is planned for the end of 2023.

A technological run for the cryomagnetic system is planned for the autumn of 2024. In the course of this run

ISBN: 978-3-95450-245-5 ISSN: 2226-0374 doi:10.18429/JACoW-COOL2023-FRPAM1R2

we plan to commission the following systems: general cryogenic system, cryostat system of magnets, power supplies for main magnets and quads, thermometry system of SC magnets, quench detection and energy evacuation system, power supplies for correctors, vacuum systems for the thermo-insolation and beam vacuum system, and monitoring and control systems.

Figure 9: Assembling of Collider arc magnets.

The first beam runs are scheduled at end 2024. For the first year of operation the beam energy will be limited to 2.5 GeV/u and the initial luminosity is expected to be about 10^{25} cm^{-2}s^{-1} (Fig. 10). Initially the luminosity will be set by the number of ions which can be accumulated in the Collider barrier buckets in the absence of cooling.

Table 1: Main Parameters of the Collider

Circumference	503.04 m
Maximum magnetic rigidity	45 T·m
Average residual gas pressure in beam chamber (room temperature equivalent)	$<10^{-10}$ Torr
Maximum field in dipole magnets	1.8 T
Kinetic energy of gold nuclei	1-4.5 GeV/u
Length of electron cooling section	6 m
Luminosity at the top energy	10^{27} cm^{-2} s^{-1}

Additionally to the electron cooling [17] the collider will have stochastic cooling systems capable to cool all three degrees of freedom. Beam cooling represents the key accelerator technology, which is critical for achieving the design luminosity of the complex. The electron cooling system [3] for the NICA Collider with 2.5 MeV electron energy is intended for accumulation and bunch formation at the ion kinetic energies in the range of 1.0 - 4.5 GeV/u. The cooling time of Au^{79+} ions is expected to be about 100 s at ion energy 3-4.5 GeV/u (Fig. 11). The solenoid cooling section has the length of 6 m and the magnetic field of 1 kGs. The maximum electron beam current is 1 A. Construction of the electron cooling system was started in BINP in 2016. Its commissioning will start in 2025. The stochastic cooling hardware will be installed in stages. The first stage which includes about 25% of the complete system is expected to be installed by the end of 2025.

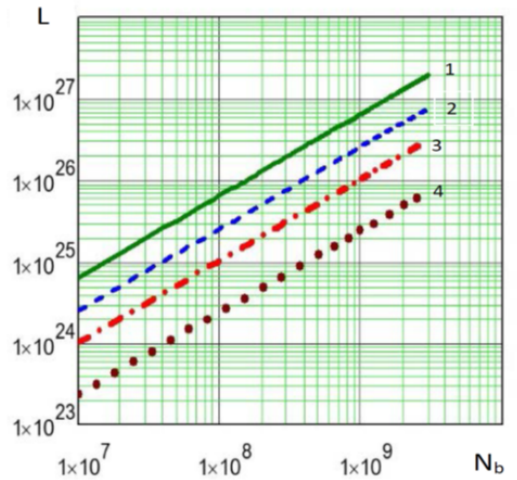

Figure 10: Dependence of luminosity on the number of ions per bunch at different energies (1) 4.5 GeV/u, (2) 3 GeV/u, (3) 2 GeV/u, (4) 1 GeV/u.

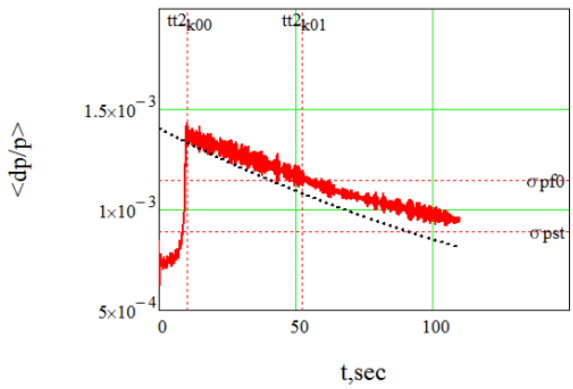

Figure 11: Dependence of ion momentum spread on time at RF3 bunching and cooling for cooling time of 100 s.

A usage of collider electron cooling system is critical to reach the ion momentum spread of $\delta p/p \approx 10^{-3}$ and bunch length of 0.6 m. Due to these reasons an effort to achieve the design luminosity of $L = 10^{27}$ sm^{-2}s^{-1} is expected to start after complete commissioning of RF3 and electron cooling and an installation of the full energy extraction from Nuclotron in 2026.

REFERENCES

[1] G. V. Trubnikov *et al.*, "Project of the Nuclotron-based Ion Collider Facility (NICA) at JINR", in *Proc. EPAC'08*, Genoa, Italy, Jun. 2008, paper WEPP029, pp. 2581-2583.

[2] V.D. Kekelidze R. Lednicky, V.A. Matveev, *et al.*, "Three stages of the NICA accelerator complex", *Eur. Phys. J. A*, v.52:211, pp.390, 2016. doi:10.1088/1742-6596/668/1/012023

[3] "Technical Project of NICA Acceleration Complex", Dubna, 2015.

ISBN: 978-3-95450-245-5 ISSN: 2226-0374 doi:10.18429/JACoW-COOL2023-FRPAM1R2

[4] A.V. Butenko, O.I. Brovko, A.R. Galimov, *et al.,* "NICA Booster a superconducting synchrotron of new generation", *UFN*, vol. 193, No. 2, pp. 206-225, 2023.

[5] M. Kapishin, "The fixed target experiment for studies of baryonic matter at the Nuclotron (BM@N)", *EPJ Web of Conferences,* vol. 182, 02061, pp.1-6, 2018. doi:10.1051/epjconf/201818202061

[6] M. Patsyuk, T. Atovullaev, A. Corsi, *et al*., "BM@N data analysis aimed at studying SRC pairs: one-step single e-nucleon knockout measurement in inverse kinematic out a 48 GeV/c ^{12}C nucleus", *Phys. Part. Nuclei Lett*., vol. 52, no. 4, pp. 631-636, 2021.

[7] E. Syresin, O. Brovko, A. Butenko, *et al.,* "NICA ion collider and plans of its first operation", in *Proc. IPAC'22*, Bangkok, Thailand, June 2022, pp.1819-1821. doi:10.18429/JACoW-IPAC2022-WEPOPT001

[8] O.I. Brovko, A.V. Butenko, A.P. Galimov, *et al.,* "NICA ion collider and its acceleration complex", in *Proc. IPAC'23*, Venice, Italy, June 2023, pp. 616-619. doi:10.18429/JACoW-IPAC2023-MOPL043

[9] "Multi-purpose detector MPD", https://nica.jinr.ru/projects/mpd.php

[10] "Spin Physics detector (SPD)", https://nica.jinr.ru/ru/projects/spd.php

[11] E.D. Donets, E.E. Donets, D.E. Donets, *et al.*, "ESIS ions injection, holding and extraction control system", *EPJ Web of Conferences* 177, vol. 5, p. 08002, 2018. doi:10.1051/epjconf/201817708002

[12] A.V. Butenko, V.S. Aleksandrov, E.E. Donets, *et al.*, *"*The Heavy Ion Injector at the NICA Project", in *Proc. LINAC'14*, Geneva, Switzerland, 2014, pp. 1068-1070.

[13] E.M. Syresin, "Injection in NICA booster with electron cooling", *Phys. Part. Nucl. Lett.*, vol. 12, No. 4, pp. 591-596, 2015. doi:10.1134/S1547477115040226

[14] M. Bryzgunov *et.al*., "Status of the electron cooler for NICA booster and results of its commissioning", in *Proc. COOL'19*, 23-27 September, Novosibirsk, Russia, pp. 22-25, doi:10.18429/JACoW-COOL2019-TUX01

[15] L.V. Zinovyev *et. al*., "Start of Electron Cooling System for the NICA Booster", *Phys. Part. and Nucl. Lett.,* ISSN 1547-4771. vol. 15, No. 7, 2018, pp. 745-748. doi:10.1134/S1547477118070737

[16] E. Syresin, A. Baldin, A. Butenko, *et al.,* "NICA synchrotrons and their cooling systems", in *Proc. COOL'21,* Novosibirsk, Russia, 2021, pp. 1-5. doi:10.18429/JACoW-COOL2021-S101

[17] M.I. Bryzgunov *et.al*., "Status of the High-Voltage Electron-Cooling System of the NICA Collider", *Phys. Part. Nucl. Lett.*, vol. 17, vol. 4, pp. 425-428, 2020. doi:10.1134/S1547477120040135